Engineering

Materials Science fields

Okayama University *Year* 2008

Primary cultures of chick osteocytes retain functional gap junctions between osteocytes and between osteocytes and osteoblasts

Hiroshi Kamioka* Yoshihito Ishihara† Hans Ris‡

Sakhr A. Murshid** Yasuyo Sugawara††

Teruko Takano Yamamoto‡‡ Soo-Siang Lim§

*Department of Orthodontics and Dentofacial Orthopedics, Okayama University Graduate School of Medicine, Dentistry, and Pharmaceutical Sciences, kamioka@md.okayama-u.ac.jp

†Department of Orthodontics and Dentofacial Orthopedics, Okayama University Graduate School of Medicine, Dentistry, and Pharmaceutical Sciences

‡Department of Zoology and Integrated Microscopy Resource, University of Wisconsin

**Department of Orthodontics and Dentofacial Orthopedics, Okayama University Graduate School of Medicine, Dentistry, and Pharmaceutical Sciences

††Department of Orthodontics and Dentofacial Orthopedics, Okayama University Graduate School of Medicine, Dentistry, and Pharmaceutical Sciences

‡‡Department of Orthodontics and Dentofacial Orthopedics, Okayama University Graduate School of Medicine, Dentistry, and Pharmaceutical Sciences

§National Science Foundation

Microsc. Microanal. 13, 108–117, 2007
DOI: 10.1017/S143192760707016X

Microscopy AND Microanalysis

Primary Cultures of Chick Osteocytes Retain Functional Gap Junctions between Osteocytes and between Osteocytes and Osteoblasts

Hiroshi Kamioka,[1,*] Yoshihito Ishihara,[1] Hans Ris,[2] Sakhr A. Murshid,[1] Yasuyo Sugawara,[1] Teruko Takano-Yamamoto,[1] and Soo-Siang Lim[3]

[1]*Department of Orthodontics and Dentofacial Orthopedics, Okayama University Graduate School of Medicine, Dentistry, and Pharmaceutical Sciences, Okayama, Japan*
[2]*Department of Zoology and Integrated Microscopy Resource, University of Wisconsin, Madison, WI 53706-1794, USA*
[3]*National Science Foundation, Arlington, VA 22230, USA*

Abstract: The inaccessibility of osteocytes due to their embedment in the calcified bone matrix *in vivo* has precluded direct demonstration that osteocytes use gap junctions as a means of intercellular communication. In this article, we report successfully isolating primary cultures of osteocytes from chick calvaria, and, using anti-connexin 43 immunocytochemistry, demonstrate gap junction distribution to be comparable to that found *in vivo*. Next, we demonstrate the functionality of the gap junctions by (1) dye coupling studies that showed the spread of microinjected Lucifer Yellow from osteoblast to osteocyte and between adjacent osteocytes and (2) analysis of fluorescence replacement after photobleaching (FRAP), in which photobleaching of cells loaded with a membrane-permeable dye resulted in rapid recovery of fluorescence into the photobleached osteocyte, within 5 min postbleaching. This FRAP effect did not occur when cells were treated with a gap junction blocker (18α-glycyrrhetinic acid), but replacement of fluorescence into the photobleached cell resumed when it was removed. These studies demonstrate that gap junctions are responsible for intercellular communication between adjacent osteocytes and between osteoblasts and osteocytes. This role is consistent with the ability of osteocytes to respond to and transmit signals over long distances while embedded in a calcified matrix.

Key words: osteocytes, osteoblasts, gap junctions, intercellular communication, dye coupling, FRAP

Introduction

Osteocytes are the most numerous cells in bone and they form an extensive three-dimensional structural network via their slender processes (Kamioka et al., 2001; Sugawara et al., 2005). After gap junctions were first identified between osteocytes and between osteocytes and osteoblasts (Doty, 1981), it became clear that osteoblasts and osteocytes may be physiologically connected, because gap junctions are involved in intercellular communication between coupled cells.

A gap junction is constructed from transmembrane proteins that form structures called connexons. A connexon is composed of a ring of six identical protein subunits called connexin (Cx). When the connexons in the plasma membranes of two adjacent cells are aligned, they form a continuous aqueous channel through which small molecules ($<$1 kD) may pass (Flagg-Newton et al., 1979; Schwarzmann et al., 1981).

Cx43 is the predominant gap junction protein expressed by bone cells (Jones et al., 1993; Ilvesaro et al., 2000). Gap junction channels allow intercellular transmission of signaling ions and second messenger molecules and have been thought to play several functions in bone, including the transmission of mechanical and chemical signals from one area of bone to another and the ability of the cellular network to initiate a coordinated response to external stimuli (Schiller et al., 1992; Xia & Ferrier, 1992; Donahue et al., 1995; Vander Molen et al., 1996; Jorgensen et al., 1997). However, there is little direct evidence that osteocytes are functionally coupled via gap junctions.

Experimentation in osteocyte biology has been hindered by inaccessibility of osteocytes due to their embedment in calcified matrix and difficulties in isolating osteocytes from bone. Progress has been made by the establishment of an osteocytic cell line, MLO-Y4 (Kato et al., 1997). Yellowley et al. (2000) showed functional gap junctional communication between MLO-Y4 cells as well as MLO-Y4 cells and the osteoblastic cell line, MC3T3-E1, as determined by calcein

Received May 17, 2006; accepted October 2, 2006.
*Corresponding author. E-mail: kamioka@md.okayama-u.ac.jp

dye transfer after cell parachuting. To date, however, the functional coupling of gap junctions has not yet been demonstrated in osteocytes isolated directly from bone tissue. In this study, we demonstrate the distribution of gap junctions in osteocytes of chicken calvaria (*in vivo*) and showed evidence that gap junctions are indeed functional in osteocytes isolated from the same tissue and grown in culture. This study builds on the foundation of our previous study (Tanaka-Kamioka et al., 1998), which provided the first detailed characterization of the cytoskeleton of these osteocytes and new insights into the structural organization of the osteocytes and their processes. The demonstrated retention of functional gap junctions in this experimental model system shows that the network of osteocyte process formed in culture can also function as a true communication network, not just a structural one.

Materials and Methods

In Vivo Cx43 Staining of Bone Cells in Chick Calvaria

Gap junction localization in chick calvaria was determined by immunostaining using a mouse monoclonal antibody specific for residues 252–271 of Cx43 (Zymed Corp., South San Francisco, CA). Actin staining with fluorescently labeled Alexa594-phalloidin (excitation wavelength = 595 nm; emission wavelength = 615 nm, Molecular Probes, Inc., Eugene, OR) was used to delineate cellular outlines of osteoblasts and osteocytes. Sixteen-day-old chick calvariae were fixed with 3% paraformaldehyde in phosphate-buffered saline (PBS) for 10 min and then permeabilized by 0.5% saponin in PBS for 10 min. The fragments were rinsed and stained for 24 h at 4°C with a 1:200 dilution of Cx43 monoclonal antibody in PBS containing 1% bovine serum albumin (BSA), after which they were rinsed in PBS. After reaction with the Alexa488 conjugated secondary antibody (excitation wavelength = 495 nm; emission wavelength = 519 nm, Molecular Probes, Inc.) for mouse IgG in PBS containing 1% BSA, the fragments were again rinsed and incubated overnight in a 1:200 dilution of Alexa594-phalloidin (Molecular Probes, Inc.) in PBS containing 1% BSA. After rinsing with PBS, the samples were embedded in fluorescence mounting medium (Dako, Carpeteria, CA) containing 1 mg/ml p-phenylenediamine dihydrochloride (Sigma, St. Louis, MO), then viewed immediately. Osteocytes in chick calvaria and localization of Cx43 were visualized with a FLOUVIEW FV500 confocal laser scanning microscopy system (Olympus, Tokyo, Japan), using 0.5-μm optical slices through the 60-μm-thick specimen. Extended depth images were reconstructed from 20 optical slices from the mineralized upper surface of the osteoblast layer to 5 μm in depth using image analysis software in FLOUVIEW FV500.

Isolation of Chick Bone Cells

Osteocytes were isolated from 16-day-old fetal chicken calvariae after removal of the periosteum by sequential digestions with collagenase and treatment with EDTA, as described previously (Tanaka-Kamioka et al., 1998), but with minor modifications. After removing the periosteum, calvariae were dissected free of the noncalcified peripheries and marrow-developing areas. These were then cut into small pieces and treated with 1 mg/ml collagenase type I (Sigma Chemical Co.) in 10 mM HEPES buffer (pH 7.4) to remove soft tissue. The residual bone pieces were further treated with 5 mM EDTA in PBS containing 0.1% BSA, followed by treatment with collagenase. The released cells were filtered through an 8.0-μm Nucleopore carbonate filter (Costar) and plated on poly-D-lysine and fibronectin-coated cover glasses (Becton Dickinson Labware). This procedure resulted in up to 90% purity of osteocytes. For the microinjection studies with Lucifer Yellow, cells after the second collagenase treatment were collected and mixed with cells from the first collagenase treatment, which contains an osteoblasts/stromal cell population, to yield a population with an approximately 1:1 ratio of osteoblasts/stromal cells and osteocytes. For these studies, the presence of osteoblasts was desirable because their larger size is more conducive to successful microinjection.

Cx43 Staining of Isolated Primary Bone Cells

Isolated bone cells from chick calvaria were fixed with 3% paraformaldehyde in PBS for 7 min, then permeabilized by 0.5% saponin in PBS for 10 min. After three washes with PBS, the cells were incubated with anti-Cx43 overnight at 4°C, washed, and incubated in FITC-antimouse IgG conjugate (Cappel Research Products, Durham, NC) at 37°C for 30 min. The cover glass was washed twice in PBS and subsequently mounted on glass slides with Aqua-poly mount (Polysciences, Inc., Warrington, PA). Cells were viewed with a 100× fluorescence objective mounted on an inverted microscope. Fluorescence and phase contrast images were acquired with a FLOUVIEW FV500 confocal laser scanning microscopy system (Olympus).

High-Resolution Scanning Electron Microscopy (HRSEM)

Some field-emission scanning electron microscopes are capable of achieving 2–3-nm resolution at low accelerating voltages and are powerful tools for fine structural resolution of cell structures and their physical relationships (Ris, 1985). Isolated osteocytes were plated on #2 cover glasses that were coated with poly-D-lysine and fibronectin. Cells were fixed with 2% glutaldehyde in 0.1 M HEPES buffer (pH 7.4) for 10 min at room temperature. For preservation of the membrane surface, they were postfixed in McDonald's osmium–potassium ferricyanide mixture: 0.5% OsO_4 plus 0.8% K_3Fe (CN) for 15 min, washed in buffer, and immersed in 0.15%

tannic acid for 1–2 min. After having been rinsed in water, the preparations were dehydrated in ethanol and critical point dried. They were then Argon ion sputter-coated with a thin layer of platinum and imaged with the high-resolution in-lens HRSEM (S-900; Hitachi, Tokyo, Japan) at the Madison Integrated Microscopy Resource at 1.5-kV accelerating voltage.

Dye Coupling Studies

Intercellular communication between bone cells was examined by dye coupling studies, using (1) microinjection of Lucifer Yellow and (2) fluorescence replacement after photobleaching (FRAP) analysis.

Microinjection of Lucifer Yellow

Lucifer Yellow CH (Molecular Probes), a small molecule of 457 MW that is able to pass through gap junctions, was dissolved in 150 mM LiCl buffered with HEPES (pH 7.4). For injections, 20 mM Lucifer Yellow were backfilled in glass needles and microinjected into the cytoplasm of osteoblastic cells using a micromanipulator (Leitz, Germany). After microinjection, the cells were washed with fresh medium containing 1% FBS to remove extracellular dye. The dye was excited at 450–490 nm, and the emitted light was visualized at 515 nm. Cells were viewed with a 20× epifluorescence objective mounted on an inverted microscope. Fluorescence and phase-contrast images were acquired with a cooled charge couple device (Photometrics, Ltd., Tucson, AZ), controlled by Oncor Image software (Oncor, Inc., Gaithersburg, MD).

FRAP Analysis

The effect of drug treatment on gap junctional communication was monitored with a FLOUVIEW FV500 confocal laser scanning microscopy system using FRAP analysis (Wade et al., 1986). Cells on coverslips were viewed in a chamber constructed from a 35-mm plastic dish with a viewing window cut in its base, over which a cover glass was glued across the window with adhesive grease. The cells on cover glasses were exposed for 20 min to 1 mM 5-carboxyfluorescein diacetate, acetoxymethyl ester (CFDA-AM; Molecular Probes, Inc.), a membrane-permeable dye, in Dulbecco's phosphate-buffered saline (Gibco) for 15 min at 37°C, then washed 20 min in buffer to remove excess dye. By this time, all cells in the culture were fluorescent. Following collection of a control image of the cells, the dye was photochemically bleached in one cell to a level sufficient to observe fluorescence recovery without causing cell damage. Images were acquired, and redistribution of fluorescence was analyzed immediately afterward and at 1-min intervals thereafter. At least 10 osteocytes were analyzed in each experiment. The percentage of the fluorescence was calculated relative to the control fluorescence intensity of the cells before photobleaching.

Treatment of Osteocytes with 18 Alpha-Glycyrrhetinic Acid

18 Alpha-glycyrrhetinic acid (18 alpha-GA; Sigma), a reversible inhibitor of gap junctional intercellular communication (Davidson & Baumgarten, 1988) was dissolved in DMSO, mixed directly in the culture medium (30 μM), and applied to the cells 4 h before photobleaching experiments. In some experiments, 18 alpha-GA was present in the medium during the period of FRAP treatment, whereas in others, 18 alpha-GA was removed before FRAP to reverse the effects of the drug.

Identification of Bone Cells

Osteocytes were immunologically identified by 1:20 dilution of OB 7.3, an mAb osteocyte-specific monoclonal antibody kindly provided by Dr. P.J. Nijweide, University of Leiden, The Netherlands (Nijweide & Mulder, 1986). Cells were washed with PBS and incubated with mAb OB 7.3 in alpha-MEM at 37°C for 30 min. After several rinses with PBS, the cells were fixed with 3% paraformaldehyde (Ladd Research Industries, Inc., Burlington, VT) in PBS for 10 min at room temperature. Then, the cells were treated with Texas Red-antimouse IgG (Vector Lab, Burlingame, CA) for 30 min at 37°C.

Osteoblasts were identified by their alkaline phosphatase (ALPase) activity. For histochemical analysis, cells were sequentially stained for ALPase activity by using naphtol AS-MX phosphate and fast red violet LB salt. Also after the images of mAb OB7.3 staining osteocytes had been taken, the cells were tested for ALPase activity by incubating for 20 min with a mixture of 0.1 mg/ml naphtol AS-MX phosphate, 0.5% N, N-dimethylformamide, and 0.6 mg/ml of fast red violet LB salt in 0.1 M TRIS-HCl (pH 8.5), at room temperature.

Statistical Analysis

For comparisons within cells in FRAP experiments, the Mann–Whitney U test was used. Probability levels of $p < .05$ were considered significant. Significance tests were calculated using statistical analysis software (StatView, SPSS, Chicago, IL).

Results

Gap Junction Localization, Morphology, and Distribution in Chicken Calvaria

First, we examined the *in vivo* localization and distribution of gap junctions from chicken calvaria, the tissue from which we planned to isolate the osteocytes. Anti-Cx43 immunolabeling was used to identify gap junctions, and the binding of fluorescently labeled phalloidin to actin filaments delineated cellular outlines of osteoblasts and osteo-

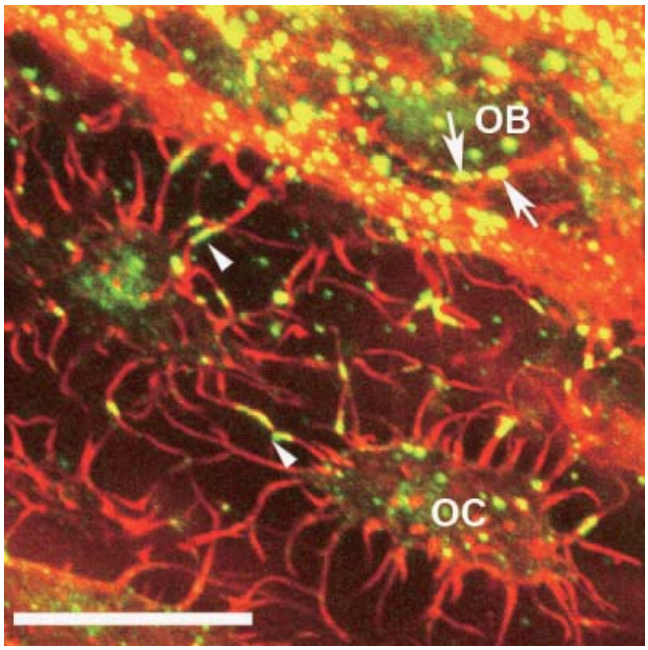

Figure 1. Extended focus images of calvaria fragment stained with Alexa488 anti-Cx43 (green channel) and Alexa594-conjugated phalloidin (red). In the red channel, actin filaments delineate cellular outlines of osteoblasts (OB) and osteocytes (OC). Green channel shows Alexa488 localization of Cx43, which appears yellow in image because of overlap with the red actin filaments. Extended focus image was reconstructed from 20 optical slices obtained from the mineral facing surface of osteoblast layer to 5 μm in depth. Arrow indicates Cx43 reactivity between osteoblasts. Arrowheads indicate Cx43 reactivity between osteocytes. Bar, 10 μm.

cytes. In the extended focus image (Fig. 1), Cx43 immunoreactivity was detected as linear fragments along osteocyte processes (arrowheads; Fig. 1). In general, Cx43-reactive sites between osteoblasts and between osteocytes and osteoblasts were spotlike and larger than immunoreactive sites between adjacent osteocytes (arrows; Fig. 1).

Anti-Cx43 Immunofluorescence of Primary Cultures of Osteocytes Showed Dotlike Reactivity in Osteocyte Processes That Contact Osteoblasts; HRSEM Showed Flattening of Osteocyte Processes at These Sites

Binding of fluorescently labeled phalloidin to actin filaments delineated cellular outlines of osteoblasts and osteocytes in chick calvaria (red staining in Fig. 2A). Using the same anti-Cx43 antibody, we examined gap junction distribution in primary cultures of osteocytes isolated from chicken calvaria. Dotlike regions of intense fluorescence were observed at the ends of osteocyte processes contacting a much larger osteoblast after 12 h in culture (arrows; Fig. 2A). To examine more closely these contact sites between osteocyte processes and osteoblasts, we used HRSEM. At higher magnification of the inset in Figure 2B, the tips of the osteocyte processes appeared flattened against the osteoblast membrane (Fig. 2C). This flattening of osteocyte processes may account for the generally larger and spotlike anti-Cx43 reactive sites observed between osteocytes and osteoblasts in primary culture (Fig. 2A) as well as between osteocytes and osteoblasts in chick calvaria (Fig. 1).

Anti-Cx43 Immunofluorescence Showed Discrete Reactive Sites in Osteocyte Processes That Contact Other Osteocytes; HRSEM Showed Details of Contact Regions between Osteocyte Processes

Double-label fluorescence staining using anti-Cx43 and Alexa594-phalloidin for actin filaments showed discrete reactive sites in osteocyte processes of osteocytes cultured for 3 h (Fig. 3A). The anti-Cx43-positive sites showed a variety of sizes, and sometimes line up in series in single process (arrowheads; inset in Fig. 3A). After additional incubation ($>$12 h), linear fragments of Cx43-positive sites become more common, resembling those seen in osteocytes *in vivo* (arrows in Fig. 3B).

HRSEM revealed the physical relationships between adjacent osteocyte processes. We noted that osteocyte processes often lie parallel to one another, with extended lengths of contact surface (Fig. 3C). This side-by-side apposition of the processes (region between arrowheads in the inset of Fig. 3C and in Fig. 3D) was often seen in osteocytes within 3 h of seeding on the cover glass. Other variations of contact regions between osteocyte processes were also observed. In most cases, there was flattening of processes at contact regions (Fig. 3E). Sometimes processes looped around each other (Fig. 3F).

Microinjection of Lucifer Yellow into an Osteoblast Showed Spreading of Fluorescence to Neighboring Osteocytes and Osteoblasts

If gap junctions are functional in the population of osteocytes and osteoblasts, they should serve as conduits through which small molecules such as the dye Lucifer Yellow can pass through from cell to cell. To test this hypthesis, a bone cell population of approximately equal numbers of osteocytes and osteoblasts/stromal cells was prepared. Because osteoblasts are larger and therefore more amenable to microinjection, they were the cells of choice for microinjection using Lucifer Yellow. The series of micrographs in Figure 4 are from an experiment to see if Lucifer Yellow microinjected into an osteoblast could spread to other neighboring cells. In Figure 4A, phase-contrast microscopy showed that isolated osteocytes made contact with other cells by long, slender processes. Based on morphology, an osteoblast-like cell in the same field (double arrow, Fig. 4A) was microinjected with 20 mM Lucifer Yellow. Three minutes later (fluorescence micrograph, Fig. 4B), the dye was detected not only in the injected cell (double arrow) but also

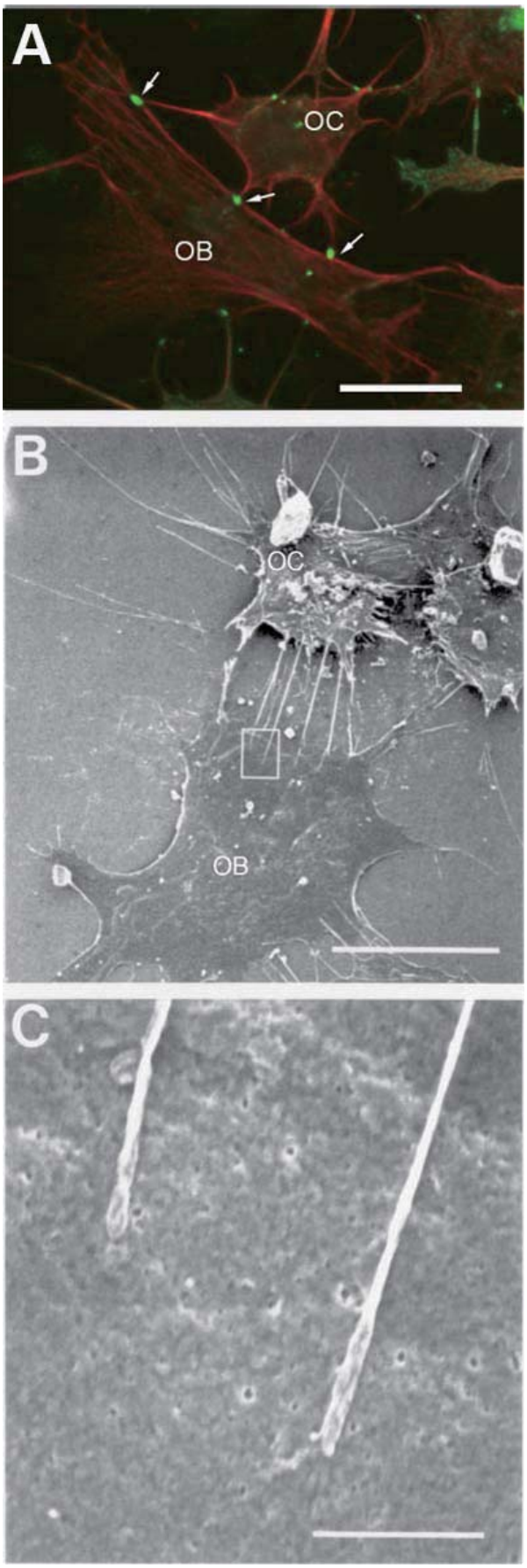

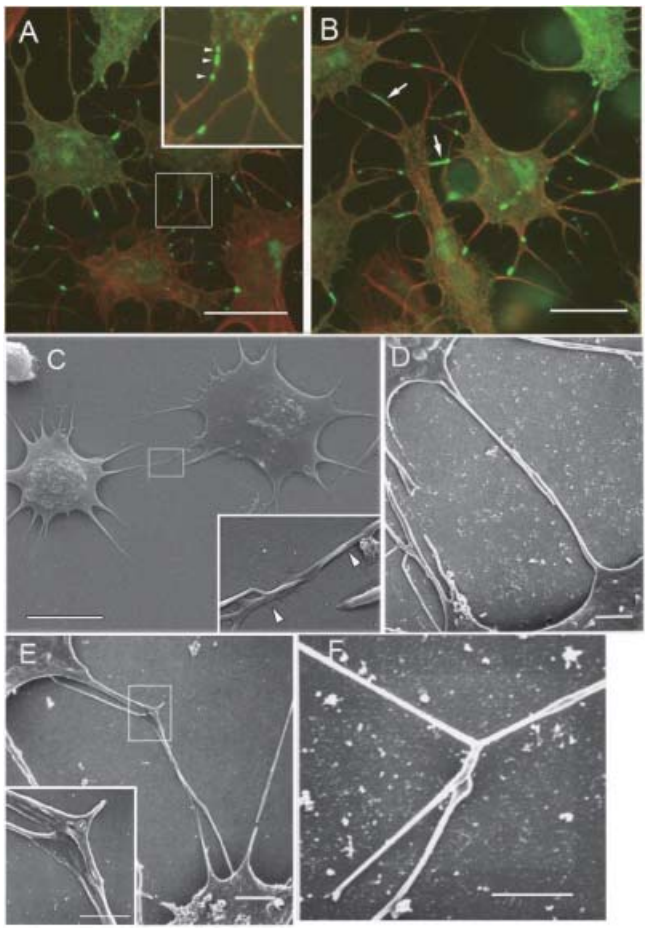

Figure 3. Double-label fluorescence staining with anti-Cx43 and Alexa594-phalloidin and HRSEM of osteocytes. Red channel shows osteocyte processes and cell body that are stained with Alexa594-phalloidin and green staining shows anti-Cx43 positive sites. **A:** Osteocytes after 3 h in culture. Cx43-reactive sites are observed as a dots or serial dots along the processes (arrowheads). **B:** Osteocytes after 12 h in culture. Cx43-reactive sites are linear along osteocyte processes (arrows). **C:** HRSEM of osteocytes 3 h after isolation. Osteocyte processes often align side by side (between arrowheads), with extended lengths of contact surface. Contact regions generally are flattened (**E**), and sometimes, processes loop around each other (**F**). Bars, 10 μm (**A**, **B**), 1 μm (**C**).

Figure 2. Double-label fluorescence staining with anti-Cx43 and Alexa594-phalloidin and HRSEM of an osteocyte and an osteoblast. Red channel shows osteocyte processes and cell body that are stained with Alexa594-phalloidin and the green channel shows anti-Cx43 positive sites. **A:** An osteocyte and osteoblasts after 12 h in culture. Strong Cx43-reactive sites were prominent on the surface of an osteoblast. **B:** HRSEM shows multiple processes from an osteocyte processes contacting an adjacent osteoblast. **C:** High magnification of inset seen in Figure 2B. OB: osteoblast, OC: osteocyte. Bars, 10 μm (**A**, **B**) and 1 μm (**C**).

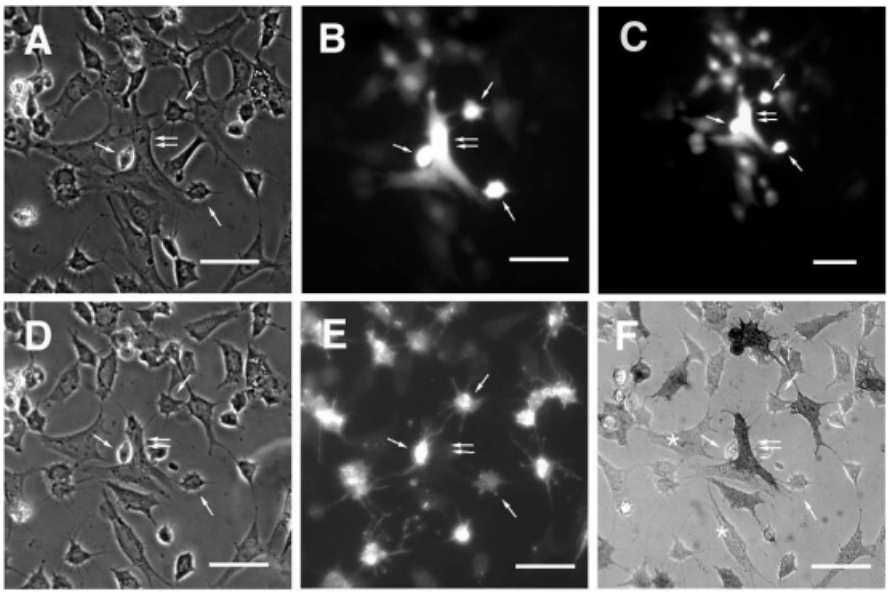

Figure 4. Dye coupling study by using microinjection of Lucifer Yellow. Phase-contrast micrograph (**A**) shows a field with osteocytes and osteoblasts/stromal cells. Based on morphology, an osteoblast (double arrow) was microinjected with 20 mM Lucifer Yellow, and fluorescence images were taken after 3 min (**B**) and 5 min (**C**). After the sample was fixed (phase, **D**), indirect immunofluorescence showed OB7.3-reactive osteocytes (**E**; single arrow). Osteoblasts were identified by ALPase activity (**F**; double arrow). Bars, 50 μm.

in surrounding cells, including some with an osteocytic morphology (single arrows, Fig. 4, cf. A and B). Five minutes after microinjection (Fig. 4C), the spread of fluorescence was seen more widely in a greater number of cells, and there was no cell-type specificity to the spread of dye.

To confirm the phenotype of the cells in the field, we then fixed the cells with paraformaldehyde (phase micrograph, Fig. 4D) and processed it for immunostaining with OB7.3 antibody to identify the osteocytes (Fig. 4E). After images were recorded, the same sample was subsequently assayed for ALPase activity to identify the osteoblasts (Fig. 4F). Some cells were both unreactive with OB 7.3 and negative for ALPase activity (asterisks, Fig. 4F), and we believe these were most likely stromal cells. Taken together, these results confirmed that the cell microinjected with dye was indeed an osteoblast, and that channels of communication between it and other cells existed to allow small molecules to pass from the microinjected cell to other osteoblasts and osteocytes in the field. In addition, we observed dye spreading from osteocytes to other osteocytes and from osteocytes to osteoblasts. These observations suggest bidirectionality of communication between osteocytes and osteoblasts rather than a specific polarity of communication from one cell type to another.

FRAP Analysis Showed Dye Coupling between Osteocytes

For this purpose, a culture consisting of mostly osteocytes was prepared for FRAP analysis. For this purpose, osteocytes were loaded for 15 min with 1 μM CFDA-AM in the medium and allowed to equilibrate, after which cells were then maintained in fresh medium without CFDA-AM. An osteocyte (arrow, Fig. 5A) was selected and photobleached. Immediately afterward (Fig. 5B) and at 1-min intervals thereafter, images were acquired and analyzed for FRAP. We observed a rapid recovery of fluorescence into the photobleached cell; within 5 min after bleaching (Fig. 5C), the fluorescence intensity returned to approximately 90% of the prebleach level (Fig. 5D). Only osteocytes with contacts with adjacent (unbleached) osteocytes showed fluorescence replacement after photobleaching. Isolated osteocytes without contact to surrounding cells did not recover fluorescence after photobleaching (data not shown).

Intercellular Communication between Osteocytes Was Inhibited by 18 alpha-GA, an Inhibitor of Gap Junctional Intercellular Communication, and Was Reversible

In these experiments, cultures were pretreated for 4 h with 30 μM 18 alpha-GA, which has been shown to block gap junctional intercellular communication. Cells were loaded with CFDA (Fig. 6A), photobleached (arrow, Fig. 6B), and postbleach images were acquired (Fig. 6C). Photobleached cells did not recover fluorescence after 5 min (Fig. 6D) or even after 30 min (data not shown). To ascertain that the above effect was not the result of 18 alpha-GA toxicity, we treated cells with 18 alpha-GA as in the above experiment and then changed the medium to fresh medium without 18 alpha-GA for recovery. After 1 h of recovery from 18 alpha-GA, the cells were loaded with CFDA-AM (Fig. 6E), a cell was photobleached (arrow, Fig. 6F), and FRAP analysis of postbleach images was conducted up to 5 min (Fig. 6G). The recovery of fluorescence in the photobleached cell showed a time dependency similar to that observed in Figure 5D (Fig. 6H).

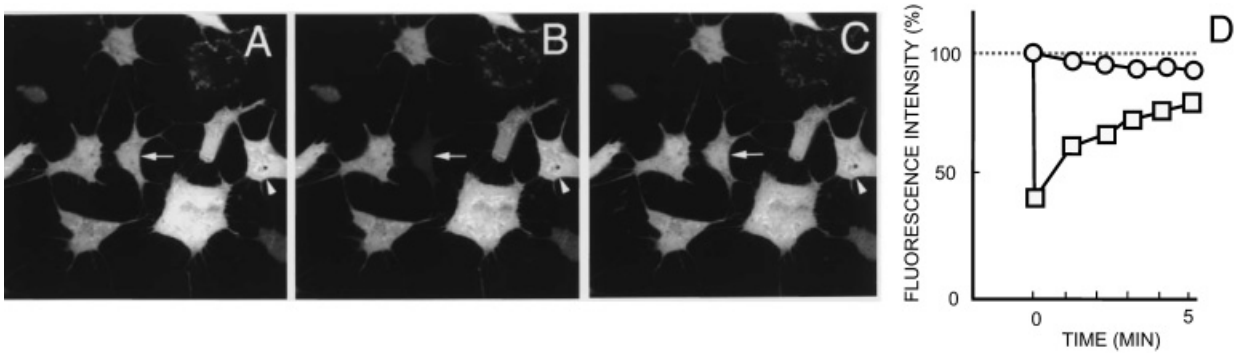

Figure 5. Dye coupling study using FRAP analysis. Osteocytes were loaded for 15 min with 1 mM CFDA-AM in the medium. After removal of excess dye, an osteocyte was selected and photobleached. Serial immunofluorescence images were taken before photobleach (**A**), immediately afterwards (**B**), and at 1-min intervals (**C**, 5 min after photobleach). A photobleached cell (arrow) and an unbleached cell (arrow head) were analyzed for FRAP (**D**). In the graph, open squares indicate the intensity of fluorescence of a photobleached cell and open circles that of an unbleached cell as the control. Zero minutes indicates immediately after photobleaching shown in **B**. The percentage of the fluorescence was calculated relative to the fluorescence intensity of the cell before photobleaching (represented at 100%). Bar, 10 μm

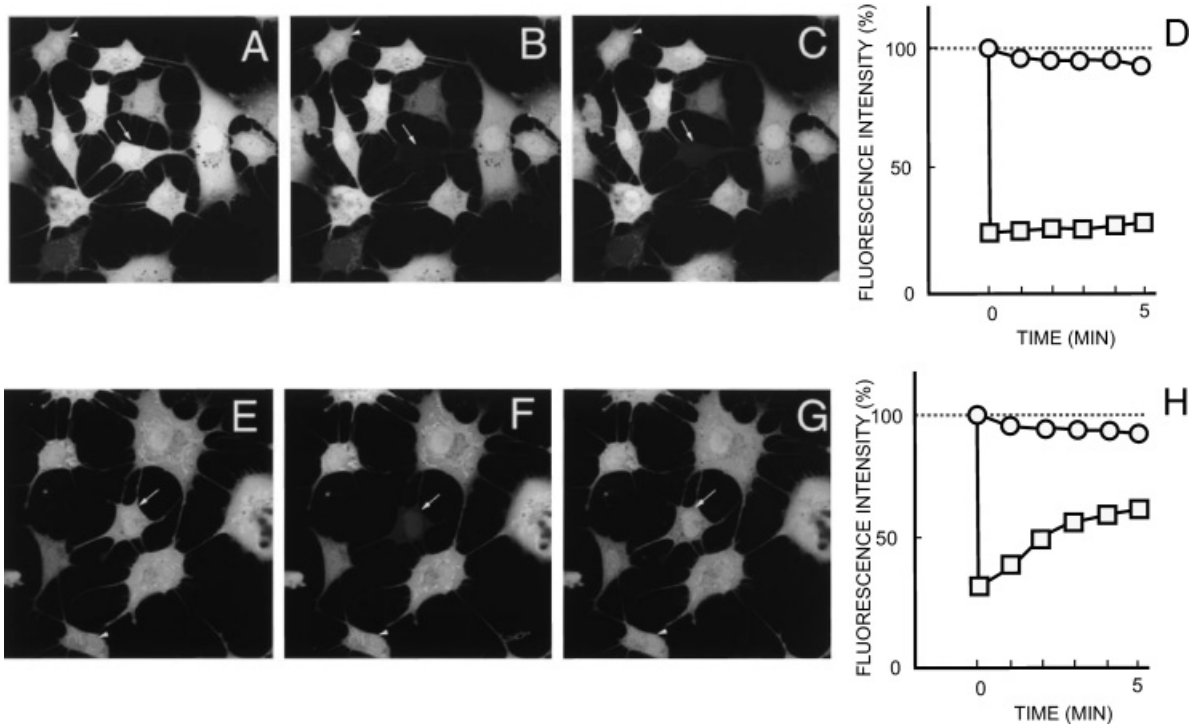

Figure 6. Inhibition of gap junctional intercellular communication by 18 alpha-GA. Osteocytes were pretreated with 30 μM 18 alpha-GA for 4 h and then loaded with 1 mM CFDA-AM in medium for 15 min. After removal of excess dye, the medium was replaced with fresh medium containing 30 μM 18 alpha-GA. An osteocyte was selected and photobleached (**B**), but no recovery of fluorescence occurred (**C**). The effects of 18 alpha-GA were reversible. When removed, photobleached cells (**F**) recover fluorescence (**G**). Serial immunofluorescence images and fluorescence recovery graphs (**D**, **H**) were obtained as in Figure 5. The percentage of the fluorescence was calculated relative to the fluorescence intensity of the cells before photobleaching (represented at 100%). Bar, 10 μm

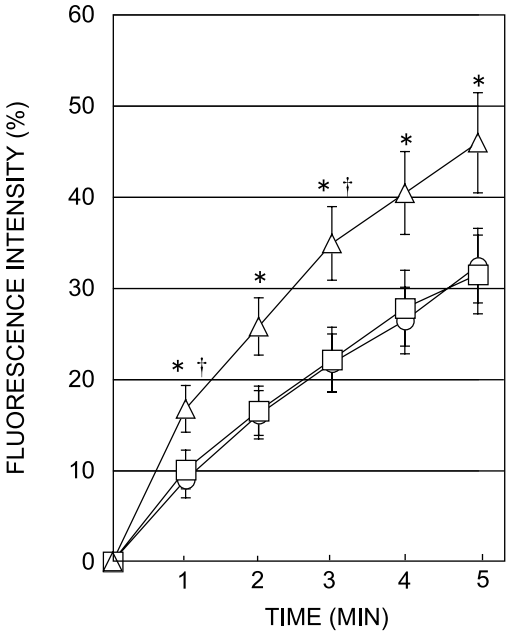

Figure 7. Recovery of fluorescence intensity between adjacent paired osteocytes (open circle), between an osteocyte and an osteoblast (open square) and between adjacent paired osteoblasts (open triangle). Time refers to minutes after photobleaching. Fluorescent intensity immediately after photobleaching was taken as 0% and that of before photobleacing was taken as 100%. Values are the means of each group with SE bars. Significant differences were observed between paired osteoblasts and paired osteocytes ($*p < .05$) as well as between paired osteoblasts and a paired osteocyte and an osteoblast ($\dagger p < .05$).

Recovery of Fluorescence between Adjacent Osteocytes, between Osteocytes and Osteoblasts, and between Adjacent Osteoblasts

In this series of experiments, FRAP analyses of osteocyte–osteocyte pairs were compared with osteocyte–osteoblast and osteoblast–osteoblast pairs. Only adjacent cells in contact with each other were selected. The analysis of paired cells allowed us to minimize differences in FRAP that may be due to differences in numbers of surrounding cells (therefore pool size of unbleached molecules) that contribute to fluorescence recovery in the photobleached cell. In both the osteocyte–osteocyte pairing and the osteocyte–osteoblast pairing, only the osteocyte partner that was photobleached and its FRAP were analyzed in the osteocyte. We did not see a significant difference in the rate of FRAP in osteocyte–osteocyte pairs, but the FRAP rate for the osteoblast–osteoblast pair was significantly faster (Fig. 7).

Discussion

The first studies on gap junctions in osteocytes were based on conventional transmission electron microscopy of demineralized bone tissue, where the bone was cut into thin slices (Doty, 1981; Jones et al., 1993). As a result, the distribution and relationship of gap junctions in context of the network of osteocyte processes were difficult to appreciate. Our immunocytochemical localization of gap junctions in calvaria provides a comprehensive and three-dimensional view of gap junction distribution in the context of the osteocyte–osteoblast network in calvaria.

In calvaria, we found that Cx43-positive plaques between osteocytes were generally small and dotlike or linear in shape. Such Cx43-rich regions were also found between adjacent osteoblasts and between osteocytes and osteoblasts. This distribution supports the concept of a functional interconnected network of cells, whereby osteoblasts on the cell surface and osteocytes deep in the bone are all interconnected and form an integrated cell system that facilitates signal integration and amplification in bone.

However, in spite of the ability to localize gap junctions *in vivo*, it is not possible to test their functionality *in situ* by present methods (FRAP and dye injection), so it becomes important to isolate and sustain the same cells in culture for experimental manipulations.

By isolating chicken calvarial osteocytes (Tanaka-Kamioka et al., 1998) and using the same connexin antibody, we confirmed that isolated primary osteocytes contain Cx43-positive sites (dotlike plaques or linear regions) similar to that observed *in vivo*. We observed their developmental patterns changing from a serial dotlike distribution of Cx43 at 3 h to predominantly linear regions of Cx43-positive sites in osteocyte processes at 12 h. We think that the linear fluorescence patterns represent the increasing side-by-side alignment of connexons from adjacent osteocytes. Such alignment of processes was often seen by HRSEM (Fig. 3C,D), and such side-by-side contact of osteocyte processes was shown by TEM to contain extended areas of membrane contact resembling gap junctions (Holtrop & Weinger, 1975). Additionally, regions of contact between osteocyte processes may take different forms. Generally there is a flattening of one or both processes (Fig. 3E), which may account for the variances in size or shape of the dotlike Cx-rich regions we see at the light microscopic level. Occasionally, some processes intertwine or loop around each other, with curvilinear regions of contact (Fig. 3F). These HRSEM images of the various physical relationships between contacting osteocyte processes may explain the variable conformations of gap junctions (linear, stacked, curvilinear, oval, and annular) that were reported in TEM studies of gap junctions in bone cells (Shapiro, 1997).

The assembly and disassembly of gap junctions have been shown to be quite dynamic. Multilabel fluorescence and electron microscopic imaging of connexin turnover in living HeLa cells reported an estimated half-life of less than 5 h for the constituent connexin (Gaietta et al., 2002). In addition, this study showed that growth of gap-junction-rich areas results from the transport of newly synthesized Cx43 to the plasma membrane, where they were incorpo-

rated into the periphery of existing gap junctions. On the other hand, older connexins were removed from the center of the gap-junction-rich regions. The ability of bone cells to assemble and disassemble gap junctions in a reasonably short time frame has important functional implications for intercellular communication.

In mixed cultures of osteocytes and osteoblasts, immunofluorescence with Cx43 confirmed the presence of gap junction proteins at sites of contact between the two cell types (Fig. 2A). HRSEM reveals that the tips of the osteocyte processes are often flattened against the osteoblast membrane. Such contact areas between osteocyte and osteoblasts have been shown by TEM to contain gap junctions (Shapiro, 1997). The demonstration that mixed cultures of isolated osteocytes and osteoblasts retained gap junction connections seen *in vivo* validates the use of such cultures to study intercellular coupling which cannot, to date, be studied *in situ*. Intercellular coupling is fundamental to an understanding of how mechanical and chemical (hormonal) signals from one area of bone influence that of another and how bone tissue works as a cellular network to provide a coordinate response to external stimuli, as seen in bone growth patterns during mechanical stress, bone repair, and other phenomena.

The gap junctions described above in the cultured cells display several behaviors that are characteristic of functional gap junctions. These are the first experiments to be conducted in primary cultures of osteocytes, in contrast to other studies that used an osteocytic cell line MLO-Y4 (Yellowley et al., 2000). The identity of cell types in these primary cultures was confirmed by mAb OB7.3 staining for osteocytes and ALPase activity for osteoblasts.

The two approaches we used (microinjection of nonpermeant fluorescent dye versus FRAP of cells loaded with membrane-permeant dye) both demonstrate the connectivity of osteocytes as well as that between osteocytes and osteoblasts. Microinjection of a nonpermeant dye into one cell predicts that it should remain within that cell, unless it is connected by open channels (e.g., gap junctions) to other cells. In such a case, the dye should spread to adjacent populations of cells. Using mixed cultures of osteocytes and osteoblasts, our results showed that a microinjected osteoblast was coupled to neighboring osteoblasts and osteocytes in contact with it, but that adjacent, noncontiguous cells were not. As the dye spread outward from the microinjected cell, it did not exhibit cell type specificity, that is, it passed from osteoblast to osteocyte (or vice versa) or from osteocyte to osteocyte. Such experiments do not, however, provide direct evidence that the spread of dye occurred through gap junctions.

Our second approach, FRAP, addresses the question of whether this cell–cell communication occurs across gap junctions. Our FRAP data indicate that dye CFDA-AM does indeed move from cell to cell via gap junctions, and that its transport can be reversibly blocked by gap junction blockers. Cells that do not show contacts with other cells do not recover fluorescence when bleached. In contrast to the previous microinjection method, this approach does not cause a change in cell volume that might change cellular equilibrium.

From FRAP analysis we demonstrated that 5 min after photobleaching, there was significant movement of unbleached dye molecules from adjacent osteocytes to result in a 90% return of prebleach levels of fluorescence (Fig. 5). These observations were comparable to results from FRAP analysis of photobleached osteoblastic MC3T3-E1 cells (Shiokawa-Sawada et al., 1997).

It is assumed that the rate of FRAP in the bleached cell depends on factors that affect movement of unbleached molecules from the adjacent unbleached cell. These may include numbers of gap junctions and the pool size of the unbleached dye of the attached "donor" cell. In experiments using osteocyte–osteocyte pairs or osteocyte–osteoblast pairs, we find that there is no significant difference in the rate of FRAP in the bleached osteocyte even though the osteoblast is 30–40 μm in size, compared to 10–15 μm for the osteocyte. These results argue against pool size as the primary factor affecting the rate of FRAP. Instead, gap junctions at contact regions between cells may play the larger role. This is supported by the significantly faster rate of FRAP observed in the osteoblast–osteoblast pair, which show higher densities of Cx43-positive regions (data not shown). There may also be other types of connexins involved in forming junctions, as has been reported in osteoblasts (Laing et al., 2001).

The gap-junction-specific nature of the cell–cell coupling is further reinforced by the data on reagents that inhibit gap junction intercellular communication. The gap-junction inhibitor, 18-alpha GA, prevented FRAP in bleached osteocytes (Fig. 6D) and its removal reestablished the patency of these channels (Fig. 6H). These results directly demonstrate that intercellular coupling in osteocytes is dependent on gap junctions.

Conclusions

Intercellular communication in bone cells is an important area of study, but thus far, it has not yet successfully studied *in vivo*. We believe that correlative studies of *in vivo* calvarial osteocytes and osteoblasts, together with *in vitro* cultures of the same cells, is a potentially powerful combination to overcome the technical limitations imposed by the calcified bone matrix in which osteocytes are embedded. In an earlier study, we were able to show the distinctive cytoskeletal features of ostecytes (such as the localization of fimbrin to osteocyte processes) that uniquely distinguish them from osteoblasts (Kamioka et al., 2004). Our demonstration that primary cultures of calvaria osteocytes retain functional gap junctions adds significantly to their use as better models of the *in vivo* system. We believe that the current demonstra-

tion of the functional capability of primary osteocytes to form a communication network in culture will make it a well-characterized, experimental model for the investigation of the dynamics of intercellular coupling in bone tissue and the factors that contribute to, or are affected by such activities.

Acknowledgments

H.K. thanks Kayo Tanaka-Kamioka for her technical assistance in this study, conducted during H.K.'s study abroad in S.S. Lim's laboratory at the Department of Anatomy, Indiana University School of Medicine. The passing away of H. Ris was a tremendous loss to this collaboration; we deeply value his personal friendship and scientific contributions and regret that he did not see the final version of the manuscript. This study was supported in part by grants-in-aid for scientific research from the Japan Society for the Promotion of Science.

References

Davidson, J.S. & Baumgarten, I.M. (1988). Glycyrrhetinic acid derivatives: A novel class of inhibitors of gap-junctional intercellular communication. Structure–activity relationships. *J Pharmacol Exp Ther* **246**, 1104–1107.

Donahue, H.J., McLeod, K.J., Rubin, C.T., Andersen, J., Grine, E.A., Hertzberg, E.L. & Brink, P.R. (1995). Cell-to-cell communication in osteoblastic networks: Cell line-dependent hormonal regulation of gap junction function. *J Bone Miner Res* **10**, 881–889.

Doty, S.B. (1981). Morphological evidence of gap junctions between bone cells. *Calcif Tissue Int* **33**, 509–512.

Flagg-Newton, J., Simpson, I. & Loewenstein, W.R. (1979). Permeability of the cell-to-cell membrane channels in mammalian cell junction. *Science* **205**, 404–407.

Gaietta, G., Deerinck, T.J., Adams, S.R., Bouwer, J., Tour, O., Laird, D.W., Sosinsky, G.E., Tsien, R.Y. & Ellisman, M.H. (2002). Multicolor and electron microscopic imaging of connexin trafficking. *Science* **296**, 503–507.

Holtrop, M.E. & Weinger, J.M. (1975). The ultrastructure of bone. *Ann Clin Lab Sci* **5**, 264–271.

Ilvesaro, J., Vaananen, K. & Tuukkanen, J. (2000). Bone-resorbing osteoclasts contain gap-junctional connexin-43. *J Bone Miner Res* **15**, 919–926.

Jones, S.J., Gray, C., Sakamaki, H., Arora, M., Boyde, A., Gourdie, R. & Green, C. (1993). The incidence and size of gap junctions between the bone cells in rat calvaria. *Anat Embryol (Berl)* **187**, 343–352.

Jorgensen, N.R., Geist, S.T., Civitelli, R. & Steinberg, T.H. (1997). ATP- and gap junction-dependent intercellular calcium signaling in osteoblastic cells. *J Cell Biol* **139**, 497–506.

Kamioka, H., Honjo, T. & Takano-Yamamoto, T. (2001). The three-dimensional distribution of osteocyte processes revealed by the combination of confocal laser scanning microscopy and differential interference contrast microscopy. *Bone* **28**, 145–149.

Kamioka, H., Sugawara, Y., Honjo, T., Yamashiro, T. & Takano-Yamamoto, T. (2004). Terminal differentiation of osteoblasts to osteocytes is accompanied by dramatic changes in the distribution of actin-binding proteins. *J Bone Miner Res* **19**, 471–478.

Kato, Y., Windle, J.J., Koop, B.A., Mundy, G.R. & Bonewald, L.F. (1997). Establishment of an osteocyte-like cell line, MLO-Y4. *J Bone Miner Res* **12**, 2014–2023.

Laing, J.G., Manley-Markowski, R.N., Koval, M., Civitelli, R. & Stenberg, T.H. (2001). Connexin 45 interacts with zonula occulens-1 and connexin43 in osteoblastic cells. *J Biol Chem* **276**, 23051–23055.

Nijweide, P.J. & Mulder, R.J. (1986). Identification of osteocytes in osteoblast-like cell cultures using a monoclonal antibody specifically directed against osteocytes. *Histochemistry* **84**, 342–347.

Ris, H. (1985). The cytoplasmic filament system in critical point-dried whole mounts and plastic-embedded sections. *J Cell Biol* **100**, 1474–1487.

Schiller, P.C., Mehta, P.P., Roos, B.A. & Howard, G.A. (1992). Hormonal regulation of intercellular communication: Parathyroid hormone increases connexin 43 gene expression and gap-junctional communication in osteoblastic cells. *Mol Endocrinol* **6**, 1433–1440.

Schwarzmann, G., Wiegandt, H., Rose, B., Zimmerman, A., Ben, H.D. & Loewenstein, W.R. (1981). Diameter of the cell-to-cell junctional membrane channels as probed with neutral molecules. *Science* **213**, 551–553.

Shapiro, F. (1997). Variable conformation of GAP junctions linking bone cells: A transmission electron microscopic study of linear, stacked linear, curvilinear, oval, and annular junctions. *Calcif Tissue Int* **61**, 285–293.

Shiokawa-Sawada, M., Mano, H., Hanada, K., Kakudo, S., Kameda, T., Miyazawa, K., Nakamaru, Y., Yuasa, T., Mori, Y., Kumegawa, M. & Hakeda, Y. (1997). Down-regulation of gap junctional intercellular communication between osteoblastic MC3T3-E1 cells by basic fibroblast growth factor and a phorbol ester (12-O-tetradecanoylphorbol-13-acetate). *J Bone Miner Res* **12**, 1165–1173.

Sugawara, Y., Kamioka, H., Honjo, T., Tezuka, K. & Takano-Yamamoto, T. (2005). Three-dimensional reconstruction of chick calvarial osteocytes and their cell processes using confocal microscopy. *Bone* **36**, 877–883.

Tanaka-Kamioka, K., Kamioka, H., Ris, H. & Lim, S. (1998). Osteocyte shape is dependent on actin filaments and osteocyte processes are unique actin-rich projections. *J Bone Miner Res* **13**, 1555–1568.

Vander Molen, M.A., Rubin, C.T., McLeod, K.J., McCauley, L.K. & Donahue, H.J. (1996). Gap junctional intercellular communication contributes to hormonal responsiveness in osteoblastic networks. *J Biol Chem* **271**, 12165–12171.

Wade, M.H., Trosko, J.E. & Schindler, M. (1986). A fluorescence photobleaching assay of gap junction-mediated communication between human cells. *Science* **232**, 525–528.

Xia, S.L. & Ferrier, J. (1992). Propagation of a calcium pulse between osteoblastic cells. *Biochem Biophys Res Commun* **186**, 1212–1219.

Yellowley, C.E., Li, Z., Zhou, Z., Jacobs, C.R. & Donahue, H.J. (2000). Functional gap junctions between osteocytic and osteoblastic cells. *J Bone Miner Res* **15**, 209–217.